Major Nb/Ta Fractionation Recorded in Garnet Amphibolite Facies Metagabbro

Xing Ding,[1,*] *Yanhua Hu,*[2] *Hong Zhang,*[1,3] *Congying Li,*[1] *Mingxing Ling,*[1] *and Weidong Sun*[4,†]

1. State Key Laboratory of Isotope Geochemistry, Guangzhou Institute of Geochemistry, Chinese Academy of Sciences, Guangzhou 510640, China; 2. Zhejiang Institute of Geological Survey, Hangzhou 311202, China; 3. State Key Laboratory of Continental Dynamics, Northwest University, Xi'an 710069, China; 4. Key Laboratory of Mineralogy and Metallogeny, Guangzhou Institute of Geochemistry, Chinese Academy of Sciences, Guangzhou 510640, China

ABSTRACT

Mobilities and fractionations of high-field-strength elements, especially Nb and Ta within a subducting slab, are important for deciphering the formation of the continental crust (CC). Here we report geochemical results on an epidote garnet amphibolite facies metagabbro body in the Tongbai-Dabie orogenic belt, central China. Our samples were hydrated during prograde metamorphism of the Triassic plate subduction. Major minerals such as amphibole, garnet, rutile, and ilmenite and garnet amphibolite bulk rocks show varied and overall lower Nb/Ta and/or Zr/Hf ratios than the continental crust. Magma differentiation might have contributed to variations of Zr/Hf but not those of Nb/Ta, suggesting major Nb/Ta fractionations during plate subduction. LA-ICPMS in situ trace element analyses of amphibole and especially rutile grains exhibit obvious chemical zonations. Typically, the rutile cores are usually small with higher Nb and Ta concentrations and lower Nb/Ta ratios compared to the thick rims. Chemical and fabric characteristics of the zonations may be explained by diverse external fluid activities: the gabbro first absorbed low Nb/Ta fluids that were released during blueschist to amphibolite transformation in deeper portions of the subducting slab, followed by acquiring external fluids with elevated Nb/Ta released during amphibolite to eclogite transformation. Our results imply that fluids with low Nb/Ta released during blueschist to amphibolite transformation can be transferred to cold regions within a subducted plate and also to the mantle wedge through fluid-rock reaction. Such regions are more easily melted during further subduction, especially in the early history of the earth, providing a plausible explanation for the low Nb/Ta in the CC.

Online enhancements: supplementary tables.

Introduction

Geological processes that lead to the formation of the continental crust (CC), especially the causation of Ti-Nb-Ta anomalies (Rudnick and Gao 2003) and subchondritic Nb/Ta ratios (19.9; Münker et al. 2003), are the subject of an ongoing debate. Previous studies suggest that at least 80% of the CC was generated at convergent margins (Barth et al. 2000; Rudnick and Gao 2003), and partial melting of subducted slabs has been considered the dominant process for the formation of the CC (McDonough 1991; Rudnick et al. 2000; Barth et al. 2002; Foley et al. 2002; Xiao et al. 2006; Xiong 2006; Ding et al. 2009; Liang et al. 2009). Given that Ti, Nb, and Ta are depleted in the CC (Rudnick and Gao 2003) and that rutile is a major accessory mineral in eclogite that controls the behaviors of Ti, Nb, and Ta (Brenan et al. 1994; Green 1995; Zack et al. 2002; Xiong et al. 2005; Liang et al. 2009), melting of subducted oceanic crust in rutile-bearing eclogite facies has been proposed as the main process that formed the CC (McDonough 1991; Rudnick et al. 2000).

Experiments, however, have shown that rutile

Manuscript received May 25, 2012; accepted January 16, 2013.

* Author for correspondence; e-mail: xding@gig.ac.cn.
† E-mail: weidongsun@gig.ac.cn.

[The Journal of Geology, 2013, volume 121, p. 255–274] 0022-1376/2013/12103-0003$15.00. DOI: 10.1086/669978

preferentially incorporates Ta over Nb compared to the equilibrated melts (Foley et al. 2000; Tiepolo et al. 2000; Schmidt et al. 2004; Klemme et al. 2005; Xiong et al. 2005). Consequently, partial melting of rutile-bearing eclogite with mid-ocean ridge basalt (MORB)–like Nb/Ta ratios (17.8; Sun and McDonough 1989) should produce melts with higher Nb/Ta, which is not consistent with the known low Nb/Ta ratios (12–13) of the CC (Rudnick and Gao 2003). Foley et al. (2002) suggested that the CC formed through a low degree of partial melting of subducted slabs in the form of rutile-free amphibolites. Although the model of partial melting of rutile-free amphibolites may be reconciled with the CC's subchondritic Nb/Ta, it cannot explain other major and trace element characteristics of the CC (Rapp et al. 2003; Xiao et al. 2006; John et al. 2011). Consequently, Rapp et al. (2003) and Xiong (2006) highlighted input materials with initially subchondritic Nb/Ta in subduction zones (e.g., arc crust and special seamount basalts). These rocks, however, are not the main components subducted along convergent margins. Alternatively, Ding et al. (2009), Liang et al. (2009), and Xiao et al. (2006) proposed that cold regions of a subducting slab, hydrated by low Nb/Ta fluids released from hotter regions during blueschist to amphibolite (BAT) metamorphism, are the key to the CC's low Nb/Ta. Schmidt et al. (2009), however, argued strongly against major fractionation between Nb and Ta during subduction processes, whereas the highly varied and overall high Nb/Ta signatures of some xenolithic eclogites (Rudnick et al. 2000) were attributed to metasomatism during long-term residence in the lithospheric mantle, as recently suggested by Aulbach et al. (2008). Consequently, John et al. (2011) and Xiong et al. (2009) attributed the low Nb/Ta in the continental crust to varied conditions of partial melting processes. Notably, previous studies focused on eclogites, which usually experienced complicated dehydration and retrograde processes, so that it is not easy either to determine whether Nb/Ta fractionation happened during subduction or to determine the main process that resulted in Nb/Ta fractionation.

In this contribution, we studied Dafushan rutile-bearing garnet amphibolite to get a better understanding of high-field-strength element (HFSE; in particular Nb-Ta and Zr-Hf) mobilities and fractionations before a slab's eclogitization. Our samples are products of gabbro to epidote garnet amphibolite prograde metamorphism, which was usually triggered by hydration of gabbro (John and Schenk 2003), by subduction that released fluids from deeper depths. The Dafushan garnet amphibolite lies in a relatively cold portion of the subducted continental slice hydrated during the subduction of the South China Block (SCB) beneath the North China Block (NCB), providing a good record of subduction-released fluids. Our study found that the Dafushan metagabbro experienced long-term fluid-rock reaction during subduction, most likely triggered by diverse external fluids derived from dehydration of other regions, which resulted in major fractionation between Nb and Ta.

Geological Settings and Samples

Geological Settings. The Tongbai-Dabie orogenic belt is the middle section of the Qinling-Dabie-Sulu orogenic belt, which has the largest-known high-pressure–ultrahigh-pressure (HP-UHP) terrain and the largest preserved continental subduction zone (fig. 1*A*). It was formed by the collision between the NCB and the SCB (Li et al. 1989, 1993, 1994; Xu et al. 1992; Zhang et al. 1995; Cong 1996; Sun et al. 2002) and reached its peak metamorphism at ca. 226 ± 2 Ma (Li et al. 2000; Liu et al. 2006).

The Tongbai-Dabie orogenic belt is usually divided into three parts, from southwest to northeast: epidote-blueschist metamorphic zone, HP-UHP metamorphic zone, and Tongbai-Dabie complex rocks (fig. 1*B*; Zhang et al. 1994, 2005*a*). The Tongbai region is further divided into six lithotectonic units: the blueschist-greenschist zone, the southern eclogite zone, the Tongbai Complex, the northern eclogite zone, the Balifan tectonic mélange, and the Nanwan flysch (Liu et al. 2008*a*). Each unit is separated by a large shear zone or fault (Zhong et al. 1999), suggesting that they do not belong to the same subducted slices and consequently experienced varied subduction paths (Li et al. 2010; Liu et al. 2010). Previous studies show that portions of the HP-UHP metamorphic zone were subducted into the mantle to depths of >100 km in the Early Triassic (Zhang and Liou 1996; Ye et al. 2000; Liu et al. 2008*a*), whereas the blueschist metamorphic zone was subducted to the lower crust in the Late Triassic (Li et al. 2010) and then uplifted rapidly back to the upper CC (You et al. 2005; Zhang et al. 2005*b*, 2005*d*).

The Dafushan metagabbroic body is located in Hubei province, central China, with outcrops distributed in an area of about 8 km^2. Tectonically, it is situated in the southwestern margin of the southern eclogite zone, bounded on the south by the blueschist metamorphic zone in the Tongbai region (fig. 1*B*) and separated from the Qinling orogenic belt to the west by the Nanyang basin. The southern eclogite zone, extending east to the Hong'an

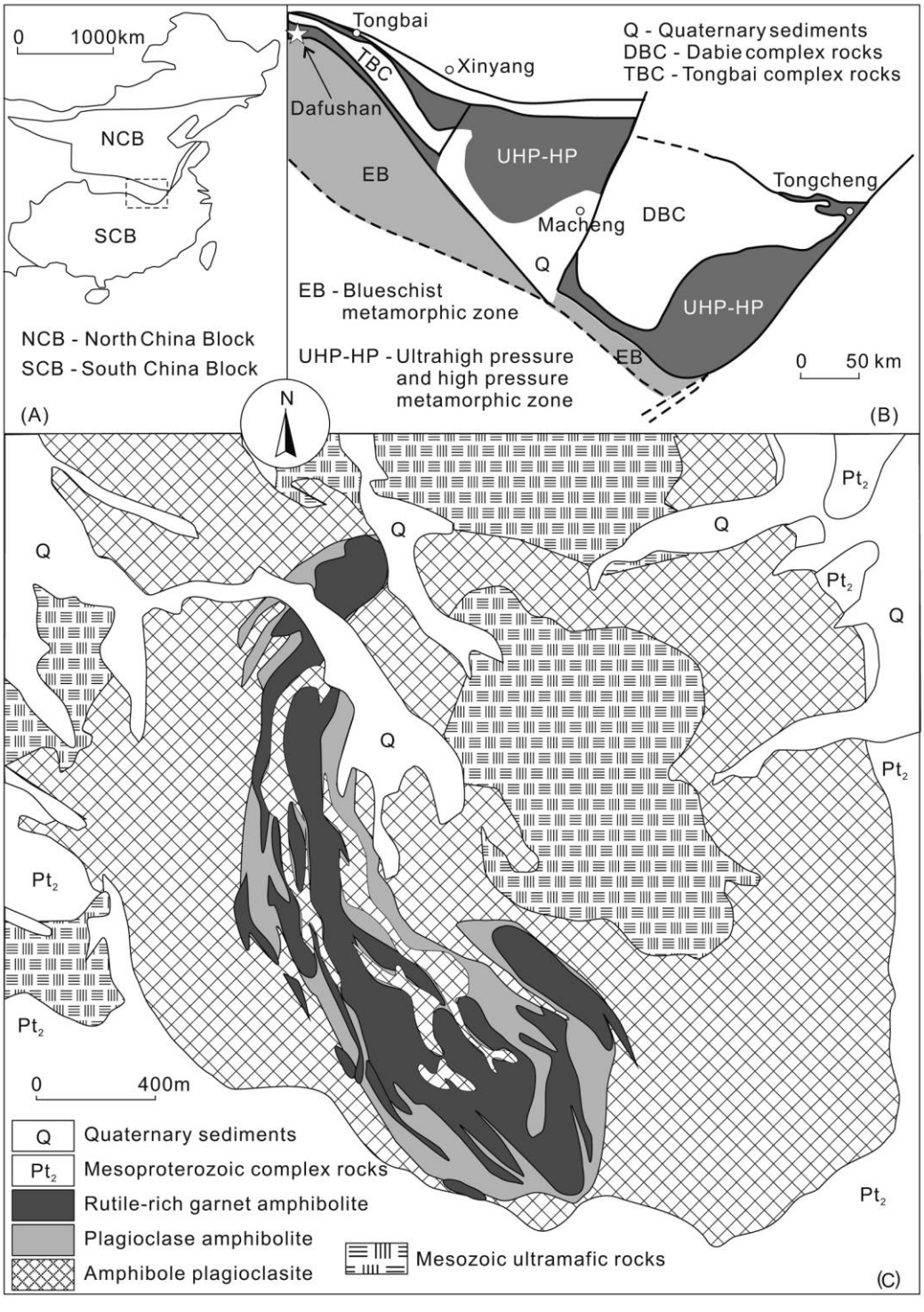

Figure 1. *A*, Simplified map of South China Block (SCB), North China Block (NCB), and collisional zone showing the location of the Tongbai-Dabie orogenic belt. *B*, Regional lithotectonic map of the Tongbai-Dabie orogenic belt, modified after Zhang et al. (1994, 2005*b*). The star represents the location of the Dafushan metagabbro, which is located in the southwestern margin of the southern eclogite zone, bounded on the south by a blueschist metamorphic zone in the Tongbai region. *C*, Simplified lithological map of the Dafushan area, modified after Xu (2006), showing a circular zonation that consists of three kinds of rutile-bearing metamorphic rocks from the exterior to the interior, i.e., amphibole plagioclasite, plagioclase amphibolite, and garnet amphibolite.

high-pressure unit (known as cold eclogite) of the western Dabie Mountains (Jahn et al. 2005), is made up of quartzofeldspathic gneiss and minor mica schist, quartzite, and marble with numerous eclogite and garnet amphibolite lenses or blocks (Liu 1996; Liu et al. 2008*a*). The largest block in the southern eclogite zone, the Dafushan metagabbro, occurs in a circular zonation intruded by Mesozoic ultramafic rocks and surrounded by Mesoproterozoic complex rocks (fig. 1*C*). SHRIMP U-Pb dating of zircon shows that the protolith of Dafushan metagabbro was formed at ca. 662 Ma (Liu et al. 2008*a*), most likely from intrusive mafic magma (Liu 1996; Xu 2006). At ca. 255 Ma, the protolith of the Dafushan metagabbro as well as other rocks in the southern eclogite zone were subducted and underwent prograde metamorphism during the subduction of the SCB beneath the NCB (Li et al. 2010; Liu et al. 2008*a*, 2010) and subsequently uplifted to shallow depths in the Middle-Late Triassic, as indicated by the muscovite $^{40}Ar/^{39}Ar$ dating of quartzite from the wall rocks that yields a plateau age of 234 ± 2 Ma and an inverse isochron age of 237 ± 3 Ma (Liu et al. 2008*a*).

The *P-T* conditions of the Dafushan metagabbro were estimated to be 520°–620°C and 6–11.5 kbar for the peak stage, according to assemblages of garnet and amphibole or rutile (Liu 1996; Xu 2006), which recorded the prograde metamorphism of gabbro to epidote garnet amphibolite. In the Tongbai region, the estimated *P-T* conditions are 530°–610°C and 17–20 kbar for the northern eclogite zone and 460°–560°C and 13–19 kbar for the southern eclogite zone (Liu et al. 2005, 2008*a*), showing a descending *P-T* tendency from northeast to southwest.

Sample Description. The Dafushan metagabbro includes three kinds of major rutile-bearing metamorphic rocks, from the exterior to the interior: weakly foliated amphibole plagioclasite, plagioclase amphibolite, and rutile-rich garnet amphibolite (figs. 1*C*, 2*A*). Rutile-rich garnet amphibolite consists mainly of amphibole (45%–60%), garnet (15%–30%), plagioclase (<5%), rutile (2%–4%), and other accessory minerals such as quartz, albite, apatite, epidote, ilmenite, pyrite, chlorite, mica, calcite, and so on (fig. 2*C*–2*F*). Plagioclase amphibolite includes amphibole (30%–50%), garnet (5%–10%), plagioclase/albite (20%–40%), epidote (~5%), titanite (~5%), rutile (1%–2%), and other accessory minerals such as albite, ilmenite, epidote, mica, chlorite, and so on, whereas amphibole plagioclasite contains mainly amphibole (<35%), albite (40%–50%), garnet (<8%), rutile (<1%), and other similar accessory minerals. Plagioclase amphibolite, and, in particular, amphibole plagioclasite and minerals therein, underwent remarkable retrogression and some deformation.

In order to exclude the effect on HFSE mobilities by retrogression, we investigated eight rutile-rich garnet amphibolite samples and their minerals from the Dafushan metagabbro. All samples showed no obvious retrogressive metamorphism and were fresh (fig. 2*B*). Mineral grains such as garnet and amphibole are well developed and show hardly any fine-grained symplectites (figs. 2*C*, 2*D*, 3) and thus are clearly different from grains in amphibolites that resulted from retrogression of ultrahigh-pressure metamorphic rocks (Zhang et al. 2005*c*; Zeng et al. 2007; Liang et al. 2009; Liu et al. 2010). A few rutile grains occasionally contain fine exsolution lamellae or needles of ilmenite (fig. 3*A*, 3*B*) and tiny xenomorphic ilmenite near the interface with the amphibole or garnet grains (figs. 2*D*, 3*B*, 3*C*). This is also different from retrograde rutile, usually rimmed or fractured or even completely replaced by ilmenite or titanite (Xiao et al. 2006; Ding et al. 2009; Liang et al. 2009; Lucassen et al. 2010). Moreover, few chloritized relict plagioclase phenocrysts (fig. 2*F*) and brown yellow relict amphiboles were observed, indicating their intrusive mafic precursor. All of these show that Dafushan garnet amphibolite did not experience significant retrogression.

Analytical Methods

Sample Preparation. All the analyses were carried out in the State Key Laboratory of Isotope Geochemistry, Guangzhou Institute of Geochemistry. Sample preparation of massive garnet amphibolites for bulk-rock analysis started with careful chipping of the samples, using a cutter to gain 0.3–1.0-cm chips of the inner parts of the core pieces. These chips were cleaned by distilled water and dried at room temperature ready for milling. Chip samples were powdered in a motorized agate mill to <200 mesh.

After each sample, the mill was cleaned by first crushing high-purity quartz sands and then milling the next chip sample, followed by blowing through an air compressor and cleaning with distilled water, to avoid cross contamination. The rock powders were heated for 3 h at 105°C to remove moisture and were preserved in a glass desiccator for sequent bulk-rock major and trace element analysis.

Major and Trace Element Analysis for Bulk Rock. Bulk-rock major and trace element analysis was performed on eight representative garnet amphibolitic samples. About two grams of dried powder

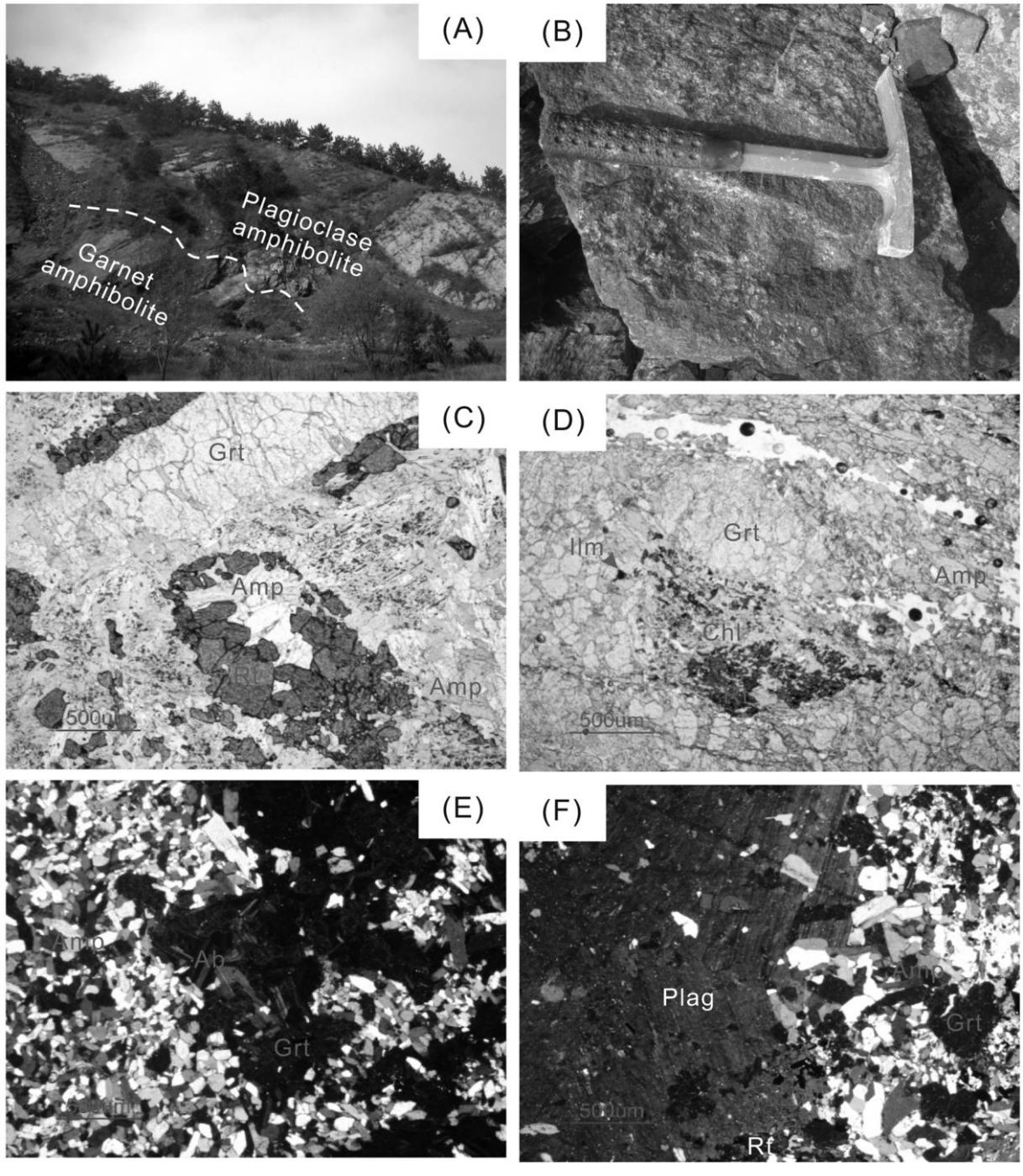

Figure 2. Field photograph and photomicrographs showing rutile-rich garnet amphibolite. *A*, A field outcrop showing the contact between dark brown garnet amphibolite and beige plagioclase amphibolite. *B*, Photograph of a hand specimen of garnet amphibolite. *C*, Plane-polarized light photomicrograph showing well-developed rutile grains of garnet amphibolite (sample DFS15-9). *D*, Plane-polarized light photomicrograph showing tiny xenomorphic ilmenite retrograded by a few rutile grains near the interface with amphibole or garnet grains (sample DFS15-3). *E*, Orthogonal light photomicrograph showing fine-grain amphibole and albite (sample DFS16-5). *F*, Orthogonal light photomicrograph showing a relict plagioclase phenocryst (sample DFS17). It, as well as relict brown hornblende phenocryst, is found in the plagioclase amphibolite, and amphibole plagioclasite is believed to be derived from the gabbroic protolith. Ab = albite; Amp = amphibole; Chl = chlorite; Grt = garnet; Ilm = ilmenite; Plag = plagioclase; Rt = rutile. A color version of this figure is available in the online edition or from the *Journal of Geology* office.

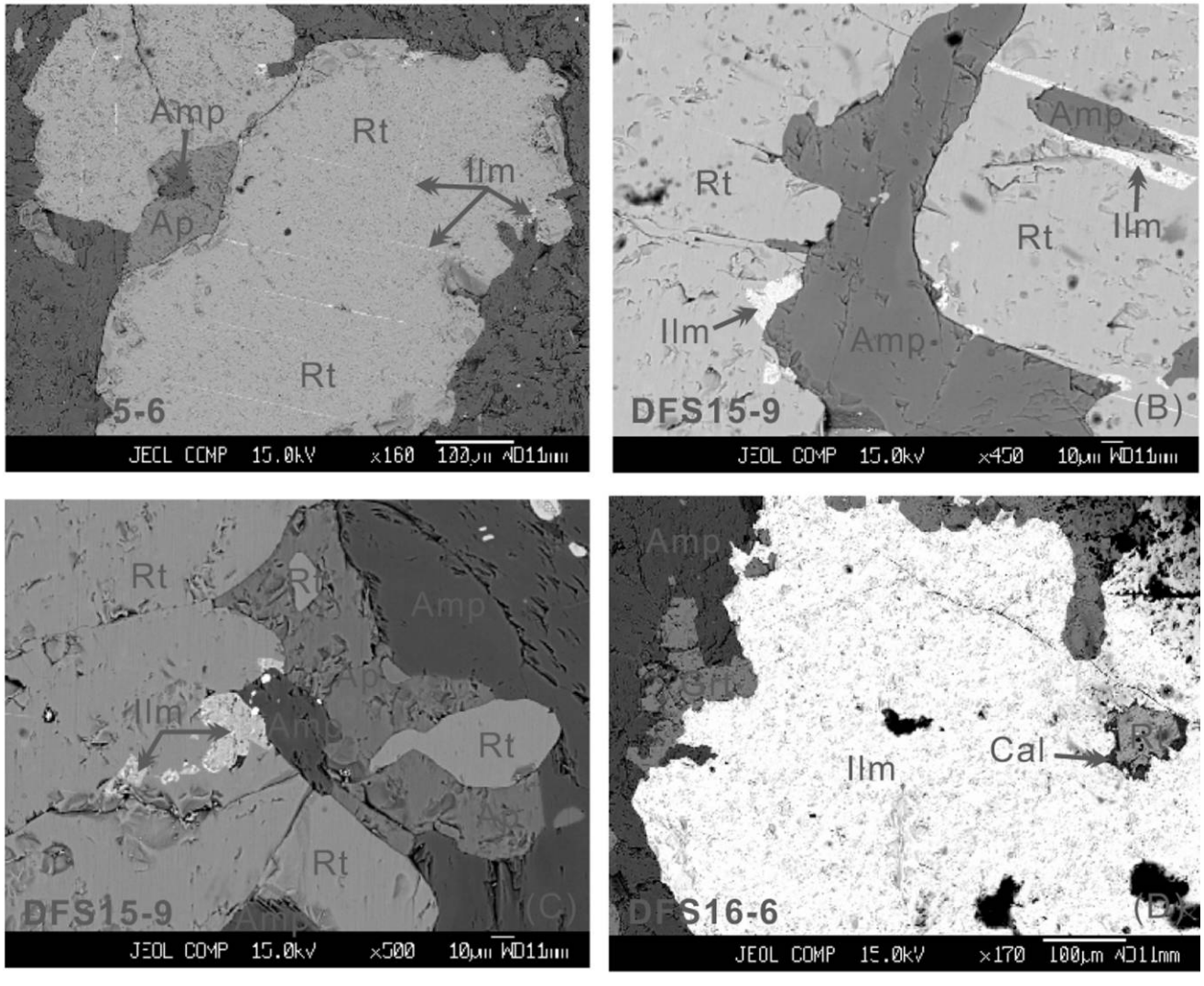

Figure 3. Back-scattered electron images showing examples of varied rutile grains and ilmenite and other minerals found in the Dafushan garnet amphibolite. Mineral grains such as garnet, amphibole, and rutile are well developed. Amp = amphibole; Ap = apatite; Cal = calcite; Ilm = ilmenite; Grt = garnet; Rt = rutile. A color version of this figure is available in the online edition or from the *Journal of Geology* office.

of each sample was first placed into a muffle furnace at 920°C for 4 h in order to determine loss on ignition and then mixed with $Li_2B_4O_7$ powder at a flux mass ratio of 1 : 8 for major element analysis and 1 : 3 for trace element analysis (Sun 2003). The mixed powder was fused at 1250°C using a V8C automatic fusion machine (Analymate) to make homogeneous glass pills. The major elements were analyzed using a Rigaku ZSX100e X-ray fluorescence spectrometry. The instrument was calibrated against international standards. Analytical precision for major elements is >1%, accuracy is >5%, and determination limits are generally >30 ppm (Ma et al. 2007). The glass pills for trace elements were performed by laser ablation inductively coupled plasma mass spectrometer (LA-ICP-MS). The LA-ICP-MS system consisted of an Agilent 7500a ICP-MS coupled with a Resonetics RESOLution M-50 ArF-Excimer laser source (λ = 193 nm), a two-volume laser ablation cell designed to avoid cross contamination and reduce background flushing time, a Squid smoothing device producing less statistic error induced by laser ablation pulses, and a computer-controlled high-precision X-Y stage (Tu et al. 2011). The ablated aerosol was carried to the ICP source with He gas. The detection limits of ICP-MS for trace elements are mostly >10 ppb, with uncertainties of 5%–10% (Liang et al. 2009; Tu et

al. 2011). In this study, laser ablation was operated at a constant energy of 80 mJ and a repetition rate of 10 Hz, with a spot diameter of 91 μm. Each analysis incorporated a background acquisition of approximately 25–30 s (gas blank), followed by 40 s data acquisition from the sample. Each analytical batch consisted of two ablations on the NIST610 standard at the beginning and the end and one on NIST612 and four glass samples in between. NIST610 was used as an external calibration standard, ^{43}Ca as an internal standard, and NIST612 as a monitoring standard to evaluate the precision and accuracy of measurements. NIST610 and NIST612 applied the reference concentrations listed in table S1, available in the online edition or from the *Journal of Geology* office. Bulk-rock samples adopted the average concentration obtained by 5–10 ablations dispersedly distributed in one glass sample. Off-line analyses and integration of background and analyzed signals and time-drift correction and quantitative calibration were performed by ICPMSDataCal (Liu et al. 2008*b*). The mean detection limit of the focused elements was 0.10 ppm for Zr, 0.01 ppm for Nb, 0.04 ppm for Hf, and 0.01 ppm for Ta. The analytical precision is mostly better than 3%, and the accuracy is <10% (table S1).

Major and Trace Element Analysis for Single Mineral. Single-mineral major element analysis in the thin sections was based on polarized light microscopy, complemented by X-ray major element mapping and back-scattered electron imaging through a JEOL JXA-8100 Superprobe. The electron probe used an accelerating voltage of 15.0 kV, beam current of 10 nA, and spot diameter of 1 μm. Both silicates and pure oxides were used as standards.

Single-mineral trace element analysis was performed on six representative garnet amphibolitic samples. Massive samples were first cut off and polished as thin sections with a thickness of up to 0.5 mm. Trace element concentrations for rutile and other mineral grains were determined by LA-ICP-MS (see above). Compositional profiles on rutile and amphibole were obtained by ablating once every 50–60 μm along the major or short axis of minerals. In this study, laser spot diameters were 24, 31, or 53 μm, depending on the size of the mineral. ^{49}Ti was used as an internal standard for rutile and ilmenite and ^{43}Ca for amphibole and garnet, while NIST610 was used as an external calibration standard and NIST612 a monitoring standard. The internal standard used 100% TiO_2 for rutile and measured major element concentration obtained by electron probe analysis for other minerals. During ablation, Si, Ti, Ca, Y, and Zr in the laser ablation signals were carefully monitored as tracers to determine the effect of exsolution or inclusion mineral during processing. Off-line analyses and integration of background and analysis signals and time-drift correction and quantitative calibration were performed by ICPMSDataCal (Liu et al. 2008*b*). The detection limit of the focused elements was 0.05–3.47 ppm for Zr, 0.01–0.44 ppm for Nb, 0.05–0.79 ppm for Hf, and 0.01–0.27 ppm for Ta, due to various diameters of laser spot used for the measurements. Reproducibility of trace element concentrations is <3%, while accuracy is mostly <15% (table S1).

Results

Mineral Chemistry. Average compositions of the representative minerals in garnet amphibolite are listed in table S2, available in the online edition or from the *Journal of Geology* office. Amphiboles in garnet amphibolites mainly show fine-grained subhedral columnar polycrystalline grains (fig. 2*E*, 2*F*), except for xenomorphic granular, included in the other minerals (fig. 3*A*–3*C*). No significant compositional differences in the amphiboles were observed; all were moderately high in FeO* (15.46–18.81 wt%), MgO (8.57–9.58 wt%), CaO (7.88–9.48 wt%), and Na_2O (3.30–4.03 wt%), indicating sodium-calcium or calcium species (Leake et al. 2003; Hawthorne and Oberti 2007). Within a single-grain amphibole, TiO_2 occasionally drops and Al_2O_3, FeO* increases. The structural formulas of amphiboles were calculated based on O = 23, and the Fe^{2+}/Fe^{3+} ratio was estimated with total cation = 13, excluding Ca, Na, and K. As seen in table S2, these amphiboles have high Al (2.009–2.508 apfu) and low Mg# values (47–53), i.e., low Mg# amphibole (Tiepolo et al. 2000). The inferred $Fe^{3+}/(Fe^{3+}+Al)$ ratio is typically <0.36. Given that ^{B}Ca varies from 1.244 to 1.505 apfu, ^{B}Na from 0.495 to 0.756 apfu, and ^{A}Na from 0.250 to 0.463 apfu, these amphiboles can be classified as sodium-calcium barroisite, dominant in garnet amphibolites, and calcium magnesio-hornblende found in sample DFS15-6 (Hawthorne and Oberti 2007).

The garnet shows xenomorphic-granular texture (fig. 2*C*–2*F*) and possesses an almandine-rich average composition. As listed in table S2, these garnets are high in Al_2O_3 (20.58–20.99 wt%) and FeO* (26.78–30.77 wt%) and low in MgO (1.47–1.79 wt%), with a low Mg# (9). Compared to those of Sulu-Dabie eclogites (Zhang et al. 2005*b*, 2005*d*), garnet in Dafushan garnet amphibolites has more almandine and fewer pyrope components ($Alm_{0.58–0.69}Grs_{0.21–0.34}Prp_{0.06–0.07}Sps_{0.02–0.03}$).

Rutile and ilmenite, which appear in the matrix

or are enclosed by other minerals (fig. 3), show relatively homogeneous major elements (table S2). Rutile contains more than 99.5 wt% TiO_2, 0.01–0.04 wt% Cr_2O_3, and 0.01–0.03 wt% Al_2O_3, whereas ilmenite includes 51.9–53.0 wt% TiO_2 and 46.2–46.3 wt% FeO^*.

Bulk-Rock Geochemistry. The major and trace element compositions of representative garnet amphibolites are listed in table S3, available in the online edition or from the *Journal of Geology* office. Garnet amphibolites from Dafushan have a small range of chemical composition and show a tholeiitic iron enrichment trend. These garnet amphibolites are low in SiO_2 (40.51%–43.97%), MgO (5.95%–7.56%), CaO (7.31%–8.88%), ALK (Na_2O+K_2O; 2.37%–3.00%), Ni (73.3–113 ppm), and Mg# (34.4–43.2) but high in $Fe_2O_3^*$ (17.83%–24.69%) and TiO_2 (1.39%–4.19%). According to the classification of igneous systems from Middlemost (1994), these garnet amphibolites are plotted into the region of olivine gabbro. In the AFM diagram (fig. 4), some of them lie in the Fe-Ti oxide-rich cumulate end, whereas others plot outside the cumulate field, which is different from typical gabbroic or ultramafic cumulates (Beard 1986). In addition, the diagram shows that these garnet amphibolites, as well as peripheral plagioclase amphibolites and amphibole plagioclasites, trend to an initially differentiated tholeiitic magma series. In figure 5, except sample DFS15-3, all of the garnet amphibolites have low rare earth element concentrations and positive Eu anomalies compared to the chondrite (fig. 5*A*) and display apparently positive Ba, Pb, Eu, and Ti anomalies and slightly positive Nb and Ta anomalies but obviously negative Th, U and Zr, Hf anomalies in the spider diagram normalized to the normal MORB (fig. 5*B*).

Notably, all eight garnet amphibolite samples display subchondritic Nb/Ta and slightly subchondritic Zr/Hf, most of which are lower than the continental crust (subcontinental). As shown in table S3, the Nb and Ta concentrations range from 1.86 to 11.6 ppm and from 0.18 to 0.75 ppm, respectively. The Nb/Ta ratio varies from 9.4 to 15.5, averaging 11.3. The Zr concentration ranges from 18.3 to 60.4 ppm, Hf from 0.52 to 1.67 ppm, and Zr/Hf from 30.7 to 36.3 (averaging 33.8).

HFSEs in Rutile. Rutile grains in Dafushan garnet amphibolite samples show moderate variations in Nb and Ta concentrations and Nb/Ta ratios, as well as highly varied Zr and Hf concentrations and Zr/Hf ratios. As shown in table S4, available in the online edition or from the *Journal of Geology* office, Nb concentrations range from 75 to 318 ppm and Ta from 4.3 to 21.2 ppm, comparable to rutile in coesite-bearing eclogites from the Roberts Victor kimberlite (Jacob et al. 2003) but much lower than those from Central Alps eclogites and garnet mica schists (Zack et al. 2002). Correspondingly, Dafushan Nb/Ta rutile ratios vary from 11.5 to 22.0, with the average of 15.2, and are mostly subchondritic. By contrast, Zr concentrations vary from 29.7 to 202 ppm and Hf from 1.8 to 8.3 ppm, with Zr/Hf ratios ranging from 12.7 to 36.5 and averaging 22.0, and again are mostly subchondritic.

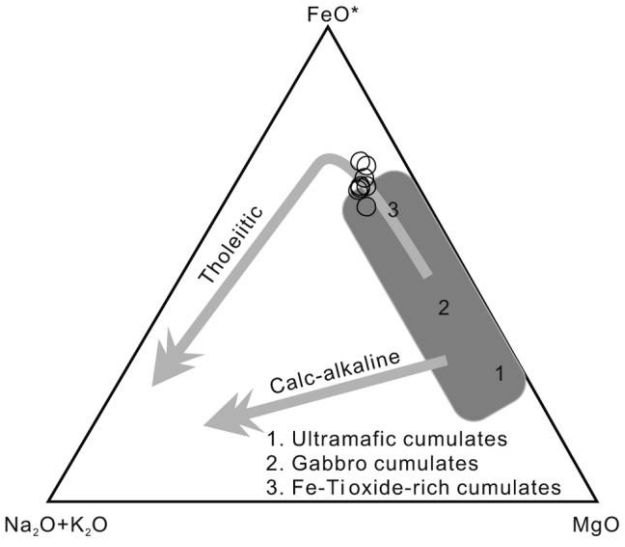

Figure 4. AFM composition of Dafushan garnet amphibolite, modified after Beard (1986) and Giannetti (1982), some of which lies in the Fe-Ti oxide-rich cumulate end whereas some plots outside the cumulate field, close to the evolution trend of initial tholeiitic magma series, indicating that the protolith is probably a differentiated gabbro, not belonging to a typical cumulate gabbro.

HFSEs in Other Minerals. As shown in table S5, available in the online edition or from the *Journal of Geology* office, ilmenite contains moderately low Nb (11.5 ppm) and Ta (1.4 ppm), with a very low Nb/Ta ratio of 8.5; garnet, amphibole, and chlorite in the Dafushan samples have very low Nb and Ta concentrations (Nb < 0.23 ppm, Ta < 0.13 ppm), a major portion of which is close to or below the detection limits. Compared to Nb and Ta, amphibole, garnet, ilmenite, and chlorite have higher concentrations of Zr and Hf (table S5). Zr concentrations in amphibole vary from 1.8 to 7.2 ppm, while Hf is <0.73 ppm (from detection limit to 0.73 ppm), with Zr/Hf ratios changing from 5.6 to 15.7. In garnet, Zr concentrations are <6.2 ppm and Hf <0.53 ppm, whereas Zr/Hf ratios are below 21.3. Similar to amphibole and garnet, the ilmenite grain ana-

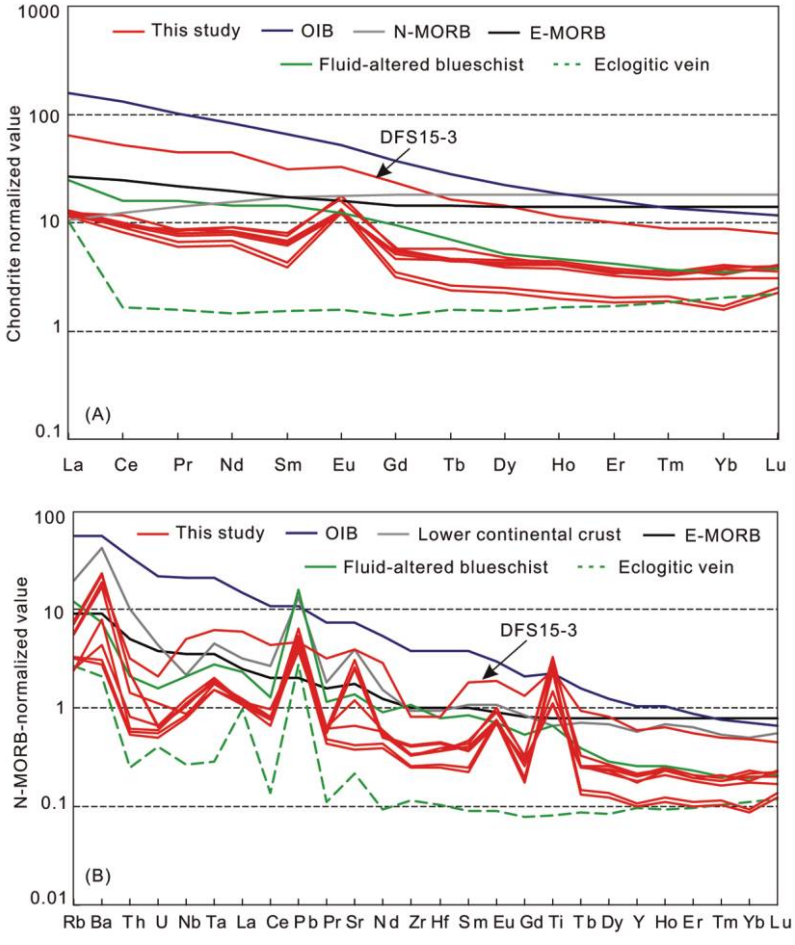

Figure 5. Chondrite-normalized rare earth element patterns and normal mid-ocean ridge basalt (MORB)–normalized trace element patterns of Dafushan garnet amphibolites, compared with fluid-altered garnet-bearing blueschist and reactive eclogitic vein from Tianshan, NW China (John et al. 2008). Normal MORB, enriched MORB, and oceanic island basalt (OIB) values are from Sun and McDonough (1989), while the lower continental crust value is from Rudnick and Gao (2003).

lyzed has 3.9 ppm Zr and 0.24 ppm Hf, with a Zr/Hf ratio of 16.6, while a chlorite grain contains 2.4 ppm Zr and low Hf. Although the trace element concentrations and ratios of these minerals could suffer from large analytical errors, there is not much doubt that they have systematically low HFSE concentrations and subchondritic Zr/Hf and Nb/Ta ratios.

Internal Chemical Zonation in Minerals. Nb and Ta of most rutile grains from the Dafushan garnet amphibolite show clear zonation, with lower Nb and Ta concentrations and higher Nb/Ta ratios in the rims (fig. 6). Moreover, intergrain variations are even more expressed than intragrain variations. To further extract the information on metamorphic evolution, the compositional profiles of several large euhedral rutile grains were carefully analyzed (table S4). As shown in figure 7, the small core has the highest concentrations of Nb and Ta, with the lowest Nb/Ta ratio. Nb and Ta decrease sharply outward whereas Nb/Ta increases gradually, resulting in systematically low Nb and Ta concentrations and high Nb/Ta ratios in the thick mantle and rim. Similarly, the highest concentrations of Zr and Hf are observed in the small core, with the lowest Zr/Hf ratios. Zr in the thick rim displays decreasing concentrations, whereas Hf in the rim shows asymmetric concentrations, resulting in asymmetric Zr/Hf in the rim.

Other minerals, such as amphibole, also show obvious trace element zonations. A compositional profile of a representative amphibole grain containing two large rutile grains shows that the concentrations of Ba, V, Zr, Hf, Rb, Cr, and Sc increase

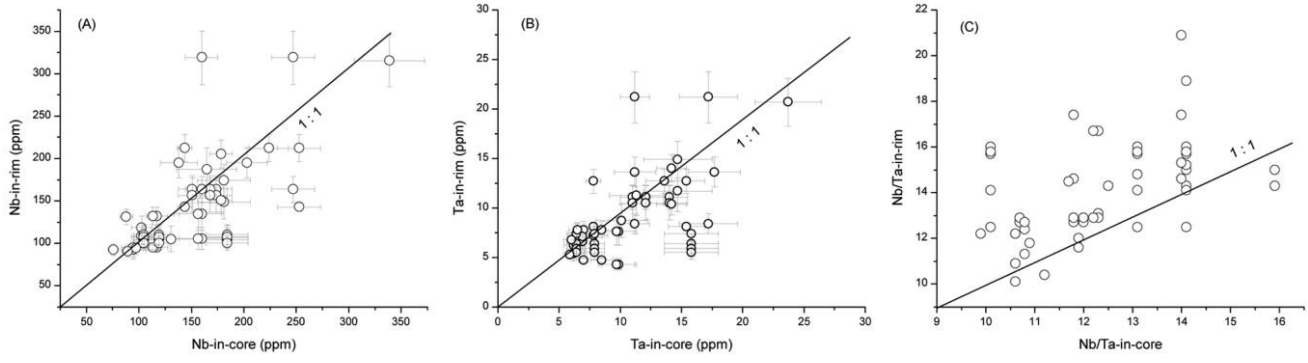

Figure 6. Nb-Ta distributions in the rims and cores of rutile grains, exhibiting intergrain variations and intragrain variations and thus obvious Nb/Ta zonations.

from the core to the rim, whereas Ti, Co, and Ni concentrations display similar tendencies from the mantle to the rim but opposite trends from the core to the mantle (AMP1-1–AMP1-8 in table S5; fig. 8).

Discussion

Effects of Crystallization on HFSE Fractionation. Either crystal fractionation during magma differentiation of the protolith or metamorphism during subduction can contribute to varied and subchondritic Nb/Ta and Zr/Hf of Dafushan garnet amphibolites. Previous studies proposed that Dafushan metagabbro was most likely derived from intrusive mafic magma (Liu 1996; Xu 2006) at the end of the Neoproterozoic (Liu et al. 2008*a*). Most of our Dafushan garnet amphibolite samples display very low trace element concentrations (fig. 5), even lower than fluid-altered blueschist in Tianshan, NW China (John et al. 2008), indicating the effect of subduction metamorphism. Note that sample DFS15-3 has the highest trace element concentrations and relatively flat pattern of trace element compared to other samples. Moreover, it shows relatively high Nb/Ta (15.5) and Zr/Hf (36.3; table S3), similar to other plagioclase amphibolites from the Dafushan metagabbro (Nb/Ta = 13.3–16.5, Zr/Hf = 37.7–43.8; X. Ding, unpub. manuscript). These suggest that this sample, as well as others with high Nb/Ta and Zr/Hf, might be closer to the precursor magma. Furthermore, they display faintly positive Eu and Ti anomalies and apparently negative Th, U, and Zr, Hf anomalies, suggesting crystal fractionation during the precursor's magma differentiation.

Nb and Ta, as well as Zr and Hf, generally do not fractionate significantly from each other during processes linked to the evolution of the earth's mantle (Jochum et al. 1986; Sun and McDonough 1989; Rudnick et al. 2000) because of their identical valence states and similar atomic radii for octahedral coordination (Shannon 1976). Also, the ratios of partition coefficients for Nb/Ta and Zr/Hf in most of major minerals occurring in mantle rocks are close to 1 (e.g., Münker et al. 2004), so fractional crystallization of these minerals cannot cause significant Nb/Ta and Zr/Hf fractionations (by a factor of >2) during general magmatism. However, fractionations of several minerals showing special crystal chemistry can obviously affect the compositions of relict melt because their partition coefficients for Nb/Ta or Zr/Hf are remarkably higher/lower than 1. For example, low Mg# amphibole segregation can significantly decrease Nb/Ta ratios of the equilibrated melts (Tiepolo et al. 2000), whereas high Mg# garnet fractionation will cause higher Nb/Ta melts (Johnson 1998; van Westrenen et al. 1999). In addition, separations of titanomagnetite (Green and Pearson 1987; Mahood and Stimac 1990) and low Mg# garnet (Hauri et al. 1994; Johnson 1998; Green et al. 2000; Klemme et al. 2002) can produce lower Zr/Hf melts. In the case of Dafushan garnet amphibolites, low Mg# amphibole and/or low Mg# garnet are metamorphic in origin, such that they do not affect magma differentiation (tables S2, S3). Segregation of some titanomagnetites during the evolution of precursor magma can decrease the Zr/Hf ratios of relict magma, which might contribute to the systematically subcontinental Zr/Hf for the Dafushan garnet amphibolites.

Accumulation of Fe-Ti oxides had involved formation of the Dafushan garnet amphibolite's protolith, i.e., gabbro (fig. 4). There is, however, no evidence that this process systematically lowered the Nb/Ta and Zr/Hf ratios of gabbro, although pre-

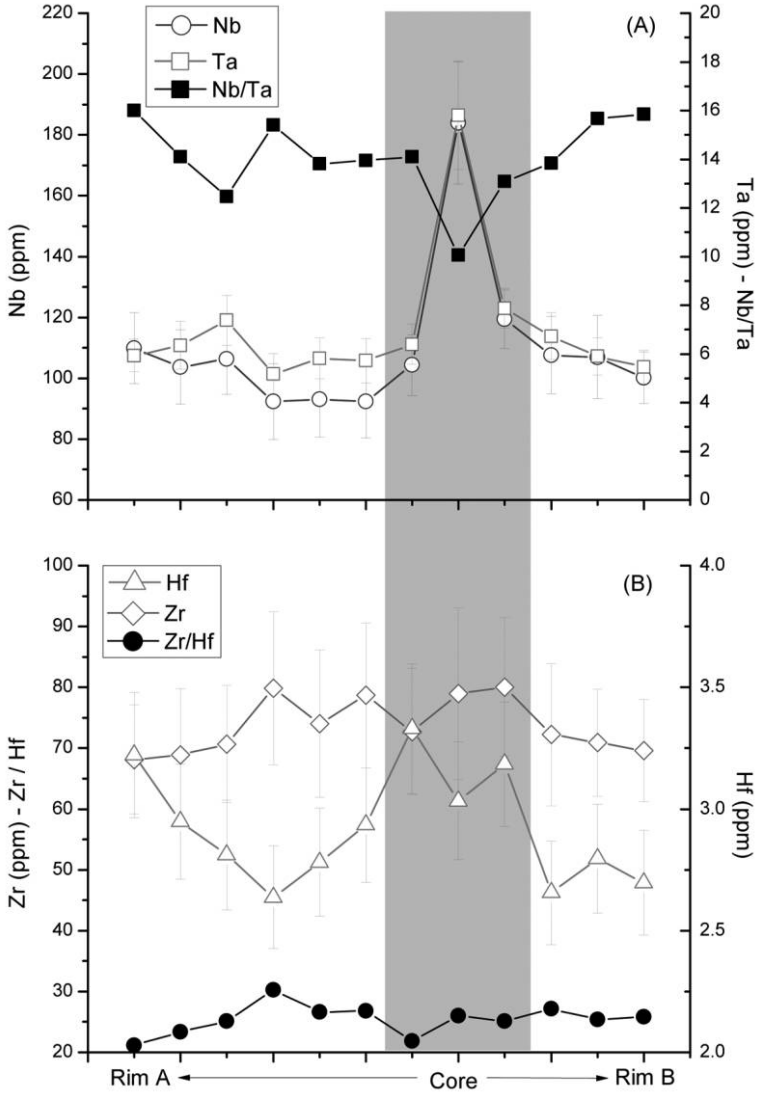

Figure 7. Compositional profile of a representative big euhedral rutile grain in sample DFS16-4, which is ablated every 50–60 μm along the major axis of a rutile. The profile shows abrupt high-field-strength element changes from the small core to the thick mantle and rim. The pattern indicates that rutile in Dafushan garnet amphibolite most likely experienced at least two episodes of fluid-mineral reactions. A color version of this figure is available in the online edition or from the *Journal of Geology* office.

vious studies proposed that Fe-Ti oxides most likely have low Nb/Ta and Zr/Hf (Green and Pearson 1987; Mahood and Stimac 1990; Münker et al. 2004). First, bulk Nb/Ta, as well as Zr/Hf, does not display distinct correlation with TiO_2 and $Fe_2O_3^*$ (fig. 9), suggesting that variations of Nb/Ta and Zr/Hf are independent of the amount of Fe-Ti oxides. Second, the magnitude of Fe-Ti oxide accumulation is limited, as shown in figure 4, in which most of samples lie outside the Fe-Ti oxide-rich cumulate field. More importantly, those amphibole plagioclasite and plagioclase amphibolites with low $Fe_2O_3^*$ (4.0–13.6 wt%) from the Dafushan metagabbro also display low Nb/Ta and Zr/Hf ratios (Nb/Ta = 10.8–12.7, Zr/Hf = 33.1–39.5; X. Ding, unpub. manuscript), which further suggests that low Nb/Ta and Zr/Hf ratios in bulk have nothing to do with accumulation of Fe-Ti oxides.

In summary, although fractional crystallization during magma differentiation might contribute to the low Zr/Hf for the Dafushan garnet amphibolites, it, as well as limited Fe-Ti oxide accumulation, cannot lead to the systematically subcontinental Nb/Ta. Therefore, Nb/Ta fractionations occurring on the whole rocks result from late metamorphism.

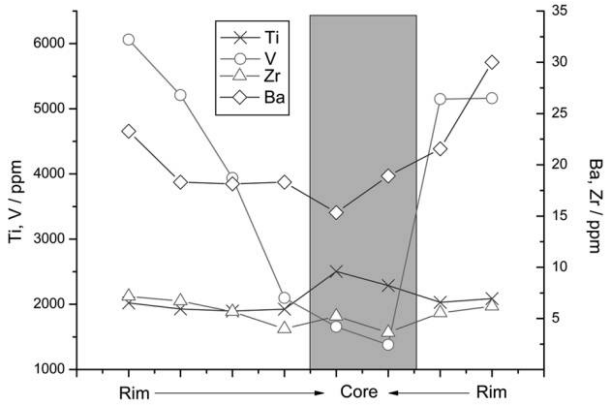

Figure 8. Compositional profile of a representative amphibole grain along a short axis showing chemical zonation in sample DFS15-3. The amphibole hosts two large rutile grains, suggesting that it was formed after or while rutile grew. Distribution patterns of Sc, Cr, Rb, Hf, and Y in amphibole are similar to those of Ba, Zr, and V, whereas Ti, Co, and Ni show the reverse distribution patterns. As in the rutile, amphibole also shows abrupt concentration changes of Zr, Hf, and other elements from the small core to the thick mantle and rim. A color version of this figure is available in the online edition or from the *Journal of Geology* office.

Nb/Ta Fractionations during Plate Subduction. Gabbro is generally dry, and internal fluids derived from the transformation among the minerals are not enough to sustain the growth of H_2O-bearing minerals such as amphibole (Hacker et al. 2003). Even eclogitic metamorphism of gabbro was attributed to hydration by external fluids, followed by dehydration (John and Schenk 2003). Previous mineralogical study on Dafushan metagabbro figured the amphibole as multigeneration minerals, mainly including primary magmatic amphibole relict and secondary barroisite (Liu 1996; Xu 2006). In our study, major amphiboles belong to sodium-calcium barroisite (table S2), even if they display obvious chemical zonation (fig. 8). Given that the barroisite usually grows in high-pressure metamorphic rocks (Hawthorne and Oberti 2007), Dafushan metagabbro was hydrated mainly during deep subduction. Moreover, the primary mantle–normalized patterns of all Dafushan garnet amphibolites resemble that of the garnet-bearing blueschist from Tianshan (NE China; fig. 5); the latter has experienced strong fluid-rock interaction due to the fluid release of subducting oceanic crust (John et al. 2008). This also implies that Dafushan metagabbro was consumingly modified by external fluids during subduction metamorphism.

Dafushan garnet amphibolites have experienced negligible retrograde metamorphism, as mentioned above, and thus provide well-preserved records of HFSE mobilities during the gabbro to amphibolite prograde metamorphism. Interestingly, our data show that the HFSE characteristics of rutile in Dafushan samples are close to those from veins of the Dabie eclogitic terrane (Nb/Ta = 10.5, Zr/Hf = 23.5; fig. 10; Xiao et al. 2006; Zhang et al. 2008) but systematically lower than rutile in eclogite (Nb/Ta = 21.3, Zr/Hf = 28.8; Ding et al. 2009; Liang et al. 2009; Schmidt et al. 2009) and amphibolite retrograded from eclogite (Nb/Ta = 17.2, Zr/Hf = 30.8; Lucassen et al. 2010). Consistently, the Nb/Ta ratios of Dafushan bulk samples are similar to those of bulk quartz veins (Nb/Ta = 10.9, Zr/Hf = 32.2; Zhang et al. 2008) but are systematically offset from those of eclogites (Nb/Ta =

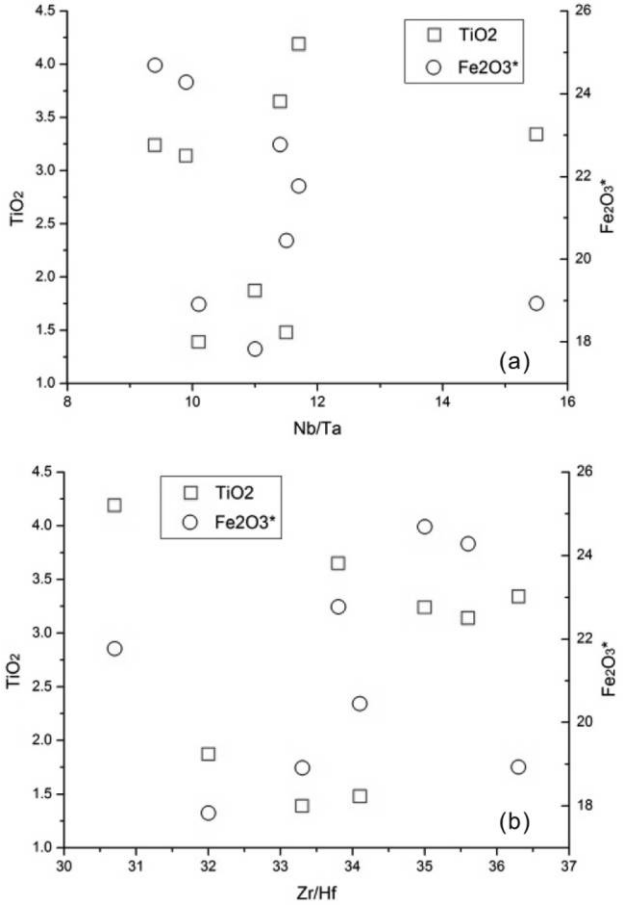

Figure 9. Plots of bulk Nb/Ta versus TiO_2, $Fe_2O_3^*$ (*a*) and bulk Zr/Hf versus TiO_2, $Fe_2O_3^*$ (*b*) from the Dafushan garnet amphibolites, suggesting that crystal fractionation or accumulation of Fe-Ti oxides had no effect on variations of bulk Nb/Ta and Zr/Hf ratios. A color version of this figure is available in the online edition or from the *Journal of Geology* office.

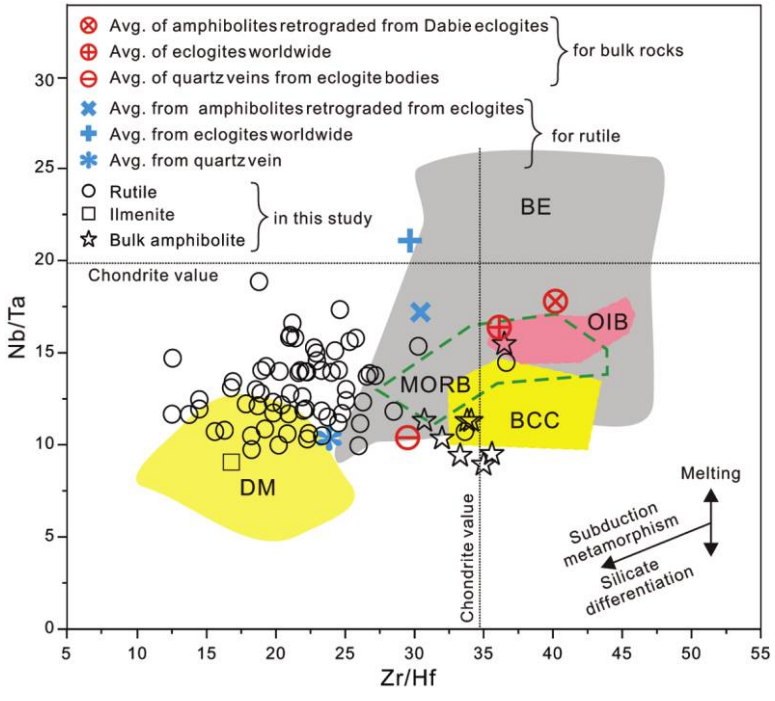

Figure 10. Plot of Zr/Hf versus Nb/Ta. Dotted lines denote values for Nb/Ta and Zr/Hf (Münker et al. 2003). Data for the major silicate reservoirs on earth are from Münker et al. (2003), with bulk eclogite from John and Schenk (2003), Liang et al. (2009), Schmidt et al. (2009), Zhang et al. (2008), and Zhao et al. (2007); average ratios of rutile from the Dabie eclogitic veins from Xiao et al. (2006) and Zhang et al. (2008); eclogites from Ding et al. (2009), Liang et al. (2009), and Schmidt et al. (2009); amphibolites retrograded from eclogites from Lucassen et al. (2010); bulk quartz veins from Zhang et al. (2008); bulk eclogites from Liang et al. (2009), Schmidt et al. (2009), Zhang et al. (2008), and Zhao et al. (2007); and bulk amphibolites retrograded from eclogites from Zeng et al. (2007) and Zhao et al. (2007). All data from rutile and bulk rocks suggest that the reaction of fluid rock can fractionate the high-field-strength elements. BCC = bulk continental crust; BE = bulk eclogitic rocks; DM = depleted mantle; MORB = mid-ocean ridge basalts; OIB = oceanic island basalts.

16.0, Zr/Hf = 36.7; Zhao et al. 2007; Zhang et al. 2008; Liang et al. 2009; Schmidt et al. 2009) and amphibolites retrograded from eclogites (Nb/Ta = 17.3, Zr/Hf = 39.3; Zeng et al. 2007; Zhao et al. 2007). These data potentially indicate two important conclusions. First, some kind of subduction zone fluid is characterized by very low Nb/Ta. This kind of fluid should be released before amphibolite to eclogite transformation (AET), because both aqueous fluids and supercritical liquids equilibrated with eclogitic rocks, regardless of whether they contain rutile, should have considerably higher Nb/Ta than the bulk rocks (Stalder et al. 1998; Kessel et al. 2005). Although partition coefficients between amphibole and subduction zone fluids are not available, we think that the fluids with low Nb/Ta should occur during BAT. Amphibole that was affected by fluids usually favors Nb over Ta (Ionov and Hofmann 1995; Marks et al. 2004), which is also supported by our data (table S5). Second, the effects of BAT and AET on Nb/Ta fractionation on the bulk rocks could erase each other, because BAT can produce higher Nb/Ta for bulk rocks and thus lower Nb/Ta for fluids, whereas AET can result in lower Nb/Ta bulk rocks and higher Nb/Ta fluids. Therefore, rocks that experienced the two transformations or that were successively altered by fluids derived from the two transformations might display fewer changes in bulk Nb/Ta ratios.

Recent studies demonstrate that Nb and Ta accompanied by Ti are fairly mobile (Xiao et al. 2006; Gao et al. 2007; Antignano and Manning 2008; John et al. 2008; Ding et al. 2009; Lucassen et al. 2010). These results indicate that high mobilities and major fractionations of Nb and Ta occur during dehydration within a subducting slab (Ding et al. 2009; Liang et al. 2009; Huang et al. 2012), which is supported by Dafushan metagabbro data. Nevertheless, Schmidt et al. (2009) argued that fluids cannot cause major Nb and Ta fractionation during subduction, based on simple mass balance esti-

mation and an assumption of equilibrium state from MORB-type eclogites. One reason leading to the debates is sample diversity and selection, because most subducted rocks such as eclogites are subject to retrogression during their ascent from great depths (Meinhold 2010). Moreover, as discussed above, information on Nb/Ta fractionation from eclogite could be erased, partially or completely, because of the opposite effects from BAT and AET. In addition, different portions of the subducting slab probably have dramatically different Nb/Ta due to the zone-refining nature of the subduction process (Xiao et al. 2006). Therefore, the average Nb/Ta values of samples from the subducting slab need to be questioned. More important, the subduction slab is not a closed system. A simple mass balance model does not work.

Formation of the Internal Chemical Zonation in Rutile. Internal zonation for HFSE in the rutile grains had previously been reported (Xiao et al. 2006; Harley 2008; Ding et al. 2009; Liang et al. 2009; Luvizotto and Zack 2009; Schmidt et al. 2009; Lucassen et al. 2010; Huang et al. 2012). Xiao et al. (2006) reported that rutile grains in quartz veins and eclogite close to quartz veins display a complicated zonation with low Nb and Ta concentrations and high Nb/Ta ratios in the thin rim mantle (named the Nb/Ta spike) and reverse Nb-Ta characteristics in the margin and speculated that the latter formed during the retrograde metamorphic stage. Schmidt et al. (2009) also found similar zonation of rutile from different orogenic MORB-type eclogites. They considered that the Nb/Ta zonation resulted from decreasing fluid activity because Ta shows higher fluid solubility than Nb or from disequilibrium mineral reactions, such as the consumption of titanite with a zonation of increasing Nb/Ta outward. Another zonation in terms of HFSE enrichment and systematically higher Nb/Ta and Zr/Hf in the small rim was reported in the rutile replaced by titanite from amphibolite, which was formed during retrograde hydration of eclogite (Lucassen et al. 2010). This kind of zonation was attributed to diffusion, based on the distribution pattern of the uniform contents in the big core and enhanced compositions in the thin rim. All rutile grains with these internal zonations show a big core and a very thin rim. The thin rims with high Nb and Ta concentrations and low Nb/Ta ratios were assigned to processes related to the retrograde metamorphism.

Rutile in this study has contrary zonations in terms of Nb, Ta, Nb/Ta, and other HFSEs, showing a small core with high Nb and Ta concentrations and low Nb/Ta ratios and a thick mantle rim with reverse characteristics, different from previous observations. These zonations cannot be formed during retrograde metamorphism. Previous experimental data for partitioning of Nb, Ta, Zr, and Hf between fluids and rutile show that under high pressure (>1 GPa) the partition coefficients generally increase as the pressure and temperature increase (Brenan et al. 1994; Stalder et al. 1998), in agreement with the pressure dependence of the Zr partition in rutile (Tomkins et al. 2007). These data indicate that with the increase of *P-T*, fewer HFSEs are incorporated into rutile from the reactive fluids, which is consistent with the systematical change of HFSE concentrations in the mantle and rim rutile and suggests prograde metamorphism.

An increase of Nb/Ta coupled with a sharp decrease of Nb and Ta from the small core to the thick rim in rutile from Dafushan garnet amphibolites cannot be explained by diffusion or disequilibrium mineral reaction during prograde metamorphism. Lattice diffusion of an element into a homogeneous lattice generally leads to smooth profiles outward and component enrichment in the grain boundary of like phase (Pearce and Wheeler 2010), as the rutile is replaced by titanite where Nb and Ta are enriched in the rim close to titanite (Lucassen et al. 2010). Although rutile growth by disequilibrium reaction of other minerals, such as titanite or pyroxene, can account for the Nb-Ta variations, it cannot easily explain why the rutile and amphibole rims are so thick (figs. 7, 8). After all, the grain size of rutile is controlled by how much material is available to be added into the grains (Pearce and Wheeler 2010). A large amount of Ti, as well as Nb and Ta, is required for continuous growth of the rim. In our opinion, external fluids played a vital role in the formation of the internal chemical zonation in rutile and amphibole. Because the Dafushan metagabbro body is now situated in the southwestern margin of the southern eclogite zone, very close to the blueschist zone, it was most likely on the upper part of the plate during subduction (Li et al. 2010). Therefore, it was easy for the metagabbro to absorb the external fluids derived from dehydration of the lower part of the plate (fig. 11), a scenario that can also plausibly explain the positive Nb-Ta and Ti anomalies for the bulk rocks in the spider diagram normalized by the normal MORB (fig. 5*B*).

Based on Nb/Ta of rutile from eclogite and quartz veins, it has been proposed that major fractionation between Nb and Ta occurs during BAT (Xiao et al. 2006). Given that amphibole favors Nb over Ta (Ionov and Hofmann 1995; Marks et al. 2004), fluids released during BAT most likely have lower Nb/Ta

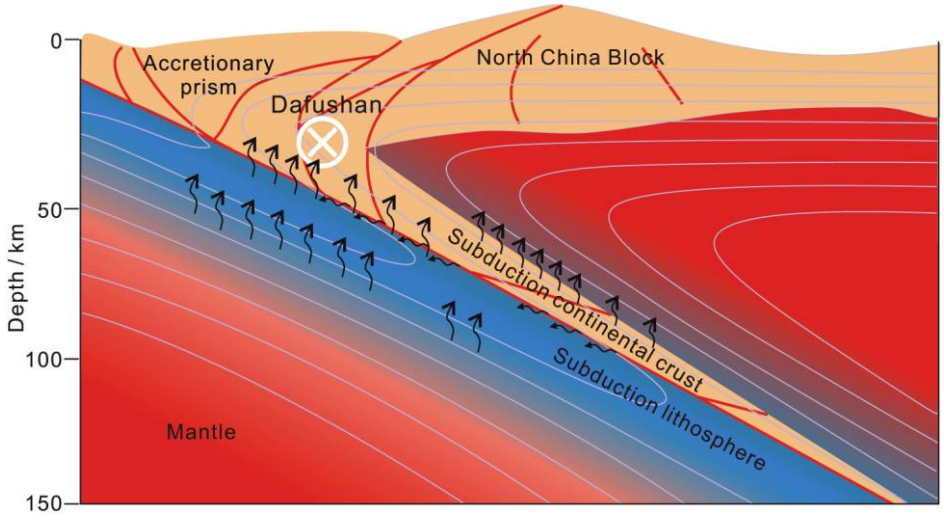

Figure 11. Schematic cross section of the sandwich structure within a subducting plate, showing two hot, dry regions and a cold, wet region in between. The thermal structure of a subducting plate is modified from Abers et al. (2006), Hacker et al. (2003), and Zack and John (2007). Given that a subducting slab is not a completely closed system, fluid activities during subduction might be complicated. Dehydration usually occurs in the hot regions, whereas hydration most likely occurs in the cold region, resulting in various high-pressure–ultrahigh-pressure rocks with Nb/Ta signatures.

(Xiao et al. 2006). Because Nb and Ta are fairly soluble in fluids in the absence of rutile (Brenan et al. 1994; Stalder et al. 1998), the fluids may contain large amounts of Nb and Ta. The low Nb/Ta fluids can be retained by amphibole or other hydrous minerals in colder and wetter regions, because of the large thermal gradient within the subducting slab (Xiao et al. 2006; Ding et al. 2009) and higher stability of amphibole in wetter conditions (Xiong et al. 2005). This explains the higher Nb and Ta concentrations coupled with lower Nb/Ta in the cores. Correspondingly, amphibolite formed after releasing low Nb/Ta fluids in hotter regions of the slab has higher Nb/Ta compared to the protolith. Fluids further released during AET should have even more elevated Nb/Ta than amphibole, because both clinopyroxene and garnet favor Ta over Nb compared to the fluids (Stalder et al. 1998; Kessel et al. 2005). In most cases, rutile appears during ATE metamorphism and thus controls the Nb and Ta in fluids. Given that rutile favors Ta over Nb (Foley et al. 2000; Tiepolo et al. 2000; Schmidt et al. 2004; Klemme et al. 2005; Xiong et al. 2005), fluids equilibrated with rutile have higher Nb/Ta ratios than source rock. The Nb and Ta concentrations in fluids are controlled by the partition between rutile and fluids in eclogite, whereas the Ti concentration is controlled by the solubility of rutile in fluids. The lower Nb and Ta concentrations in rutile rims from the Dafushan metagabbro indicate that rutile in eclogite underneath retains more Nb and Ta than Ti.

The larger high Nb/Ta rims of Dafushan rutile grains were probably due to higher initial temperatures of the gabbros, such that it collected less BAT fluids but more AET fluids. Rutile is a common mineral during high-pressure AET (Liu et al. 1998; Xiong 2006; Meinhold 2010), such that fluids released during AET tend to have lower Nb and Ta concentrations and to a less extent Ti. This explains the lower Nb and Ta concentrations coupled with higher Nb/Ta in the rims.

Implication on Formation of the Continental Crust. The most important messages we can get out of Dafushan rutile grains and garnet amphibolites are that (*a*) Nb and Ta highly fractionate from each other by long-term fluid-rock interaction during plate subduction; (*b*) there exist two kinds of fluids, with low Nb/Ta and high Nb/Ta; and (*c*) low Nb/Ta sources could be found in the subduction zone, which is mainly attributed to hydration by fluids with low Nb/Ta before eclogitization. In regard to the formation of the continental crust, hydration processes by fluids with low Nb/Ta released during BAT metamorphism are most likely the key to the low Nb/Ta in the CC (Xiao et al. 2006; Ding et al. 2009; Liang et al. 2009). Low Nb/Ta fluids can be transferred to cold regions within a subducted plate and also to the mantle wedge through fluid-rock reaction (fig. 11). In modern subduction

zones, partial melting of the mantle wedge is the main process that produces arc magmas that may eventually add to the continental crust because of cold geotherm (Hacker et al. 2003; Abers et al. 2006; Zack and John 2007). Under a hot geotherm, e.g., Archean (Foley et al. 2002; Rapp et al. 2003; Xiong 2006), partial melting of the hydrated portion within the subducting slab contributed more to the formation of the CC with low Nb/Ta (Xiao et al. 2006; Ding et al. 2009; Liang et al. 2009). Meanwhile, the residual eclogite should have even lower Nb/Ta after dehydration-induced partial melting in the presence of rutile, because rutile favors Ta over Nb compared to the melts. Therefore, further subducted eclogites should have highly varied Nb/Ta with overall suprachondritic values (because of losing subchondritic Nb/Ta components to the CC; Xiao et al. 2006), similar to those observed in xenolithic eclogites (Rudnick et al. 2000).

LA-ICP-MS In Situ Analyses for Nb and Ta in HP-UHP Rocks. It is difficult to analyze Nb, Ta, and other HFSEs in HP-UHP rocks. The most important reason is that these elements usually form resistant minerals that cannot be easily decomposed during sample digestion by ordinary methods (Sun 2003). So far, two kinds of analytical methods have been widely used for the determinations of Nb, Ta, Zr, and Hf in HP-UHP rocks and mafic rocks, including (*a*) isotope dilution with multiple collector ICP-MS coupled with fusion digestions and/or acid digestions in a high-pressure system and one-column separation methods (Münker et al. 2001, 2004; Weyer et al. 2002; Schmidt et al. 2009) and (*b*) in situ analyses with laser ablation ICP-MS using fluxed glasses with a sample/$Li_2B_4O_7$ ratio for the whole rocks and slices for minerals or inclusions (Jarvis and Williams 1993; Audétat et al. 1998; Sun 2003; Liu et al. 2008*b*; Ding et al. 2009; Liang et al. 2009).

Given that HP-UHP rocks usually experienced a complicated magmatic and metamorphic history (Sun et al. 2002; Spandler et al. 2003; Zhang et al. 2005*b*, 2007, 2008; Ernst 2010) not only in the lower CC (Liu et al. 2008*c*) and the upper mantle (Ye et al. 2000) but also during uplift to shallow depths (Schwartz et al. 2001; van der Straaten et al. 2008; Lucassen et al. 2010), bulk analysis for HP-UHP rocks could erase some important information. In this study, we observed that rutile is zoned in terms of Nb and Ta concentrations and Nb/Ta ratios and amphibole is also zoned in the components through in situ LA-ICP-MS analyses. Although these in situ analyses may not necessarily reflect the bulk composition (Schmidt et al. 2009), the most important information for Nb and Ta we can get out of HP-UHP rocks is whether Nb and Ta fractionated from each other during plate subduction. Since HP-UHP rocks exhumed to the surface are not exactly the same as those subducted (Ernst 2006), in situ analyses provide a more detailed and comprehensive image of the subduction process. From this point of view, laser ablation ICP-MS is a better choice, which provides enough resolution to identify Nb/Ta fractionation.

Conclusion

1. Most of the major minerals and bulk rocks of the Dafushan garnet amphibolite show varied and overall subcontinental Nb/Ta and/or Zr/Hf. Magma differentiation might account for variations of Zr/Hf but not Nb/Ta. Given that the Dafushan metagabbro was hydrated by external fluids released from deeper portions of the subducting slab during subduction, the varied Nb/Ta indicates high mobility and remarkable fractionations of these elements during plate subduction.

2. Rutile and amphibole exhibit obvious internal chemical zonations. The small cores of rutile have higher HFSE (Nb, Ta, Zr, and Hf) concentrations with lower Nb/Ta and Zr/Hf ratios compared to the thick rims. These zonations cannot be explained by diffusion and disequilibrium mineral reactions during the prograde or retrograde metamorphism. Instead, they can be interpreted by diverse external fluid activities: fluids released during BAT have Nb/Ta lower than the protoliths because of the presence of amphibole, followed by fluids released during AET with elevated Nb/Ta in equilibrium with garnet and omphacite and/or rutile. Because BAT can produce Nb/Ta higher for bulk rocks and thus lower for fluids, whereas AET can result in lower Nb/Ta bulk rocks and higher Nb/Ta fluids, their effects on Nb/Ta fractionations for the bulk rocks could be erased. This can plausibly explain why no major Nb/Ta fractionations in MORB-type eclogites were observed on the basis of simple mass balance estimation and an assumption of equilibrium state.

3. Long-term fluid-rock reaction during subduction metamorphism can result in low Nb/Ta characteristics in cold regions within a subducted plate and the mantle wedge. These regions are more easily melted during further subduction, especially in the early history of the earth, to produce the low Nb/Ta in the CC.

4. Bulk analysis for HP-UHP rocks could erase important information of Nb/Ta fractionations. In contrast, LA-ICP-MS in situ analyses may image a more detailed subduction process, which can tell

us when and whether Nb and Ta fractionated from each other during plate subduction.

ACKNOWLEDGMENTS

This work was supported jointly by the National Science Foundation of China (41090373 and 41002021), the Chinese Academy of Sciences (KZCX1-YW-15), and the State Key Laboratory of Isotope Geochemistry, Guangzhou Institute of Geochemistry, Chinese Academy of Sciences (GIGCAS; GIGIso-QD-12-04). We thank X. Zhou and B. Chen for discussions and Y. Liu, X. Tu, L. Chen, and G. Chen for help with the sample preparation and analyses. Also we thank H. Rollinson, F. Teng, S. Aulbach, and anonymous reviewers for detailed constructive comments and suggestions. This is contribution IS-1656 from GIGCAS.

REFERENCES CITED

Abers, G. A.; van Keken, P. E.; Kneller, E. A.; Ferris, A.; and Stachnik, J. C. 2006. The thermal structure of subduction zones constrained by seismic imaging: implications for slab dehydration and wedge flow. Earth Planet. Sci. Lett. 241:387–397.

Antignano, A., and Manning, C. E. 2008. Rutile solubility in H_2O, H_2O-SiO_2, and H_2O-$NaAlSi_3O_8$ fluids at 0.7–2.0 GPa and 700–1000°C: implications for mobility of nominally insoluble elements. Chem. Geol. 255:283–293.

Audétat, A.; Günther, D.; and Heinrich, C. A. 1998. Formation of a magmatic-hydrothermal ore deposit: insights with LA-ICP-MS analysis of fluid inclusions. Science 279:2091–2094.

Aulbach, S.; O'Reilly, S. Y.; Griffin, W. L.; and Pearson, N. J. 2008. Subcontinental lithospheric mantle origin of high niobium/tantalum ratios in eclogites. Nat. Geosci. 1:468–472.

Barth, M. G.; Foley, S. F.; and Horn, I. 2002. Partial melting in Archean subduction zones: constraints from experimentally determined trace element partition coefficients between eclogitic minerals and tonalitic melts under upper mantle conditions. Precambrian Res. 113:323–340.

Barth, M. G.; McDonough, W. F.; and Rudnick, R. L. 2000. Tracking the budget of Nb and Ta in the continental crust. Chem. Geol. 165:197–213.

Beard, J. S. 1986. Characteristic mineralogy of arc-related cumulate gabbros: implication for the tectonic setting of gabbroic plutons and for andesite genesis. Geology 14:848–851.

Brenan, J. M.; Shaw, H. F.; Phinney, D. L.; and Ryerson, F. J. 1994. Rutile-aqueous fluid partitioning of Nb, Ta, Hf, Zr, U and Th: implications for high-field strength element depletions in island-arc basalts. Earth Planet. Sci. Lett. 128:327–339.

Cong, B. L. 1996. Ultrahigh-pressure metamorphic rocks in the Dabieshan-Sulu region of China. Beijing, Science.

Ding, X.; Lundstrom, C.; Huang, F.; Li, J.; Zhang, Z. M.; Sun, X. M.; Liang, J. L.; and Sun, W. D. 2009. Natural and experimental constraints on formation of the continental crust based on niobium-tantalum fractionation. Int. Geol. Rev. 51:473–501.

Ernst, W. G. 2006. Preservation/exhumation of ultrahigh-pressure subduction complexes. Lithos 92:321–335.

———. 2010. Subduction zone metamorphism: pioneering contributions from the Alps. Int. Geol. Rev. 52: 1021–1039.

Foley, S.; Tiepolo, M.; and Vannucci, R. 2002. Growth of early continental crust controlled by melting of amphibolite in subduction zones. Nature 417:837–840.

Foley, S. F.; Barth, M. G.; and Jenner, G. A. 2000. Rutile/melt partition coefficients for trace elements and an assessment of the influence of rutile on the trace element characteristics of subduction zone magmas. Geochim. Cosmochim. Acta 64:933–938.

Gao, J.; John, T.; Klemd, R.; and Xiong, X. M. 2007. Mobilization of Ti-Nb-Ta during subduction: evidence from rutile-bearing dehydration segregations and veins hosted in eclogites, Tianshan, NW China. Geochim. Cosmochim. Acta 71:4974–4996.

Giannetti, B. 1982. Cumulate inclusions from K-rich magmas, Roccamonfina volcano, Italy. Earth Planet. Sci. Lett. 57:313–335.

Green, T. H. 1995. Significance of Nb/Ta as an indicator of geochemical processes in the crust-mantle system. Chem. Geol. 120:347–359.

Green, T. H.; Blundy, J. D.; Adam, J.; and Yaxley, G. M. 2000. SIMS determination of trace element partition coefficients between garnet, clinopyroxene and hydrous basaltic liquids at 2–7.5 GPa and 1080–1200°C. Lithos 53:165–187.

Green, T. H., and Pearson, N. J. 1987. An experimental study of Nb and Ta partitioning between Ti-rich minerals and silicate minerals at high pressure and temperature. Geochim. Cosmochim. Acta 51:55–62.

Hacker, B. R.; Abers, G. A.; and Peacock, S. M. 2003. Subduction factory. 1. Theoretical mineralogy, densities, seismic wave speeds, and H_2O contents. J. Geophys. Res. 108, doi:10.1029/2001JB001127.

Harley, S. L. 2008. Refining the P-T records of UHT crustal metamorphism. J. Metamorph. Geol. 26:125–154.

Hauri, E. H.; Wagner, T. P.; Gao, C. G.; and Grove, T. L. 1994. Experimental and natural partitioning of Th, U, Pb and other trace elements between garnet, clinopyroxene and basaltic melts. Chem. Geol. 117:149–166.

Hawthorne, F. C., and Oberti, R. 2007. Classification of the amphiboles. Rev. Mineral. Geochem. 67:55–88.

Huang, J.; Xiao, Y. L.; Gao, Y.; Zhou, Z.; and Wu, W. 2012.

Nb-Ta fractionation induced by fluid-rock interaction in subduction-zones: constraints from UHP eclogite- and vein-hosted rutile from the Dabie orogen, central-eastern China. J. Metamorph. Geol. 30:821–842.

Ionov, D. A., and Hofmann, A. W. 1995. Nb-Ta-rich mantle amphiboles and micas: implications for subduction-related metasomatic trace-element fractionations. Earth Planet. Sci. Lett. 131:341–356.

Jacob, D. E.; Schmickler, B.; and Schulze, D. J. 2003. Trace element geochemistry of coesite-bearing eclogites from the Roberts Victor kimberlite, Kaapvaal craton. Lithos 71:337–351.

Jahn, B. M.; Liu, X. C.; Yui, T. F.; Morin, N.; and Coz, M. B. 2005. High-pressure/ultrahigh-pressure eclogites from the Hong'an Block, east-central China geochemical characterization, isotope disequilibrium and geochronological controversy. Contrib. Mineral. Petrol. 149:499–526.

Jarvis, K. E., and Williams, J. G. 1993. Laser ablation inductively coupled plasma mass spectrometry (LA-ICP-MS): a rapid technique for the direct, quantitative determination of major, trace and rare-earth elements in geological samples. Chem. Geol. 106:251–262.

Jochum, K. P.; Seufert, H. M.; Spettel, B.; and Palme, H. 1986. The solar system abundances of Nb, Ta and Y and the relative abundances of refractory lithophile elements in differentiated planetary bodies. Geochim. Cosmochim. Acta 50:1173–1183.

John, T.; Klemd, R.; Gao, J.; and Garbe-Schoberg, C.-D. 2008. Trace-element mobilization in slabs due to non steady-state fluid-rock interaction: constraints from an eclogite-facies transport vein in blueschist (Tianshan, China). Lithos 103:1–24.

John, T.; Klemd, R.; Klemme, S.; Pfander, J. A.; Hoffmann, J. E.; and Gao, J. 2011. Nb-Ta fractionation by partial melting at the titanite-rutile transition. Contrib. Mineral. Petrol. 161:35–45.

John, T., and Schenk, V. 2003. Partial eclogitisation of gabbroic rocks in a late Precambrian subduction zone (Zambia): prograde metamorphism triggered by fluid infiltration. Contrib. Mineral. Petrol. 146:174–191.

Johnson, K. T. M. 1998. Experimental determination of partition coefficients for rare earth and high-field-strength elements between clinopyroxene, garnet and basaltic melt at high pressure. Contrib. Mineral. Petrol. 133:60–68.

Kessel, R.; Schmidt, M. W.; Ulmer, P.; and Pettke, T. 2005. Trace element signature of subduction-zone fluids, melts and supercritical liquids at 120–180 km depth. Nature 437:724–727.

Klemme, S.; Blundy, J. D.; and Wood, B. J. 2002. Experimental constraints on major and trace element partitioning during partial melting of eclogite. Geochim. Cosmochim. Acta. 66:3109–3123.

Klemme, S.; Prowatke, S.; Hametner, K.; and Gunther, D. 2005. Partitioning of trace elements between rutile and silicate melts: implications for subduction zones. Geochim. Cosmochim. Acta 69:2361–2371.

Leake, B. E.; Woolley, A. R.; Birch, W. D.; Burke, E. A. J.; Ferraris, G.; Grice, J. D.; Hawthorne, F. C.; et al. 2003. Nomenclature of amphiboles: additions and revisions to the International Mineralogical Association's amphibole nomenclature. Can. Mineral. 41: 1355–1370.

Li, S.; Jagoutz, E.; Chen, Y.; and Li, Q. 2000. Sm-Nd and Rb-Sr isotopic chronology and cooling history of ultrahigh pressure metamorphic rocks and their country rocks at Shuanghe in the Dabie Mountains, central China. Geochim. Cosmochim. Acta 64:1077–1093.

Li, S.; Wang, S.; Chen, Y.; Liu, D.; Ji, Q.; Zhou, H.; and Zhang, Z. 1994. Excess argon in phengite from eclogite: evidence from dating of eclogite minerals by Sm-Nd, Rb-Sr and $^{40}Ar/^{39}Ar$ methods. Chem. Geol. 112: 343–350.

Li, S. G.; Hart, S. R.; Zheng, S.; Liu, D.; Zhang, G.; and Guo, A. 1989. Timing of collision between the North and South China blocks: the Sm-Nd isotopic age evidence. Sci. Sin. B 32:1391–1400.

Li, S. G.; Xiao, Y. L.; Liou, D.; Chen, Y.; Ge, N.; Zhang, Z.; Sun, S.-S.; et al. 1993. Collision of the North China and Yangtse blocks and formation of coesite-bearing eclogites: timing and processes. Chem. Geol. 109:89–111.

Li, S. Z.; Kushy, T. M.; Zhao, G. C.; Liu, X. C.; Zhang, G. W.; Kopp, H.; and Wang, L. 2010. Two-stage Triassic exhumation of HP-UHP terranes in the western Dabie orogen of China: constraints from structural geology. Tectonophysics 490:267–293.

Liang, J. L.; Ding, X.; Sun, X. M.; Zhang, Z. M.; Zhang, H.; and Sun, W. D. 2009. Nb/Ta fractionation observed in eclogites from the Chinese Continental Scientific Drilling Project. Chem. Geol. 268:27–40.

Liu, D.; Jian, P.; Kruer, A.; and Xu, S. 2006. Dating of prograde metamorphic events deciphered from episodic zircon growth in rocks of the Dabie-Sulu UHP complex, China. Earth Planet. Sci. Lett. 250:650–666.

Liu, J. G.; Zhang, R. Y.; Ernst, W. G.; Liu, J.; and McLimans, R. 1998. Mineral paragenesis in the Pianpaludo eclogitic body, Guppo di Voltri, western Ligurian Alps. Schweiz. Mineral. Petrogr. Mitt. 78:317–335.

Liu, X. C.; Jahn, B. M.; Cui, J. J.; Li, S. Z.; Wu, Y. B.; and Li, X. H. 2010. Triassic retrograded eclogites and Cretaceous gneissic granites in the Tongbai Complex, central China: implications for the architecture of the HP/UHP Tongbai-Dabie-Sulu collision zone. Lithos 119:211–237.

Liu, X. C.; Jahn, B. M.; Dong, S.; Lou, Y.; and Cui, J. J. 2008*a*. High-pressure metamorphic rocks from Tongbaishan, central China: U-Pb and $^{40}Ar/^{39}Ar$ age constraints on the provenance of protoliths and timing of metamorphism. Lithos 105:301–318.

Liu, X. C.; Lou, Y.; and Dong, S. 2005. P-T path of low-temperature eclogites from the Tongbaishan area. Acta Petrol. Sin. 21:1081–1093.

Liu, Y. J. 1996. Further discussion on the metallization of rutile in metamorphic process. Hubei Geol. 10:26–37.

Liu, Y. S.; Hu, Z. C.; Gao, S.; Günther, D.; Xu, J.; Gao, C. G.; and Chen, H. H. 2008*b*. In situ analysis of major and trace elements of anhydrous minerals by LA-ICP-

MS without applying an internal standard. Chem. Geol. 257:34–43.

Liu, Y. S.; Zong, K. Q.; Kelemen, P. B.; and Gao, S. 2008*c*. Geochemistry and magmatic history of eclogites and ultramafic rocks from the Chinese continental scientific drill hole: subduction and ultrahigh-pressure metamorphism of lower crustal cumulates. Chem. Geol. 247:133–153.

Lucassen, F.; Dulski, P.; Abart, R.; Franz, G.; Rhede, D.; and Romer, R. L. 2010. Redistribution of HFSE elements during rutile replacement by titanite. Contrib. Mineral. Petrol. 160:279–295.

Luvizotto, G. L., and Zack, T. 2009. Nb and Zr behavior in rutile during high-grade metamorphism and retrogression: an example from the Ivrea-Verbano zone. Chem. Geol. 261:303–317.

Ma, J. L.; Wei, G. J.; Xu, Y. G.; Long, W. G.; and Sun, W. D. 2007. Mobilization and re-distribution of major and trace elements during extreme weathering of basalt in Hainan Island, South China. Geochim. Cosmochim. Acta 71:3223–3237.

Mahood, G. A., and Stimac, J. A. 1990. Trace-element partitioning in pantellerites and trachytes. Geochim. Cosmochim. Acta 54:2257–2276.

Marks, M.; Halama, R.; Wenzel, T.; and Markl, G. 2004. Trace element variations in clinopyroxene and amphibole from alkaline to peralkaline syenites and granites: implications for mineral-melt trace-element partitioning. Chem. Geol. 211:185–215.

McDonough, W. F. 1991. Partial melting of subducted oceanic-crust and isolation of its residual eclogitic lithology. Philos. Trans. R. Soc. A 335:407–418.

Meinhold, G. 2010. Rutile and its applications in earth sciences. Earth-Sci. Rev. 102:1–28.

Middlemost, E. A. K. 1994. Naming materials in the magma/igneous rock system. Earth-Sci. Rev. 37:215–224.

Münker, C.; Pfander, J. A.; Weyer, S.; Buchl, A.; Kleine, T.; and Mezger, K. 2003. Evolution of planetary cores and the earth-moon system from Nb/Ta systematics. Science 301:84–87.

Münker, C.; Weyer, S.; Scherer, E.; and Mezger, K. 2001. Separation of high field strength elements (Nb, Ta, Zr, Hf) and Lu from rock samples for MC-ICPMS measurements. Geochem. Geophys. Geosyst. 2, doi: 10.1029/2001GC000183.

Münker, C.; Worner, G.; Yogodzinski, G.; and Churikova, T. 2004. Behaviour of high field strength elements in subduction zones: constraints from Kamchatka-Aleutian arc lavas. Earth Planet. Sci. Lett. 224:275–293.

Pearce, M. A., and Wheeler, J. 2010. Modelling grain-recycling zoning during metamorphism. J. Metamorph. Geol. 28:423–437.

Rapp, R. P.; Shimizu, N.; and Norman, M. D. 2003. Growth of early continental crust by partial melting of eclogite. Nature 425:605–609.

Rudnick, R. L.; Barth, M.; Horn, I.; and McDonough, W. F. 2000. Rutile-bearing refractory eclogites: missing link between continents and depleted mantle. Science 287:278–281.

Rudnick, R. L., and Gao, S. 2003. Composition of the continental crust: treatise on geochemistry. Oxford, Pergamon, p. 1–64.

Schmidt, A.; Weyer, S.; John, T.; and Brey, G. P. 2009. HFSE systematics of rutile-bearing eclogites: new insights into subduction zone processes and implications for the earth's HFSE budget. Geochim. Cosmochim. Acta 73:455–468.

Schmidt, M. W.; Dardon, A.; Chazot, G.; and Vannucci, R. 2004. The dependence of Nb and Ta rutile-melt partitioning on melt composition and Nb/Ta fractionation during subduction processes. Earth Planet. Sci. Lett. 226:415–432.

Schwartz, S.; Allemand, P.; and Guillot, S. 2001. Numerical model of the effect of serpentinites on the exhumation of eclogitic rocks: insights from the Monviso ophiolitic massif (western Alps). Tectonophysics 342:193–206.

Shannon, R. D. 1976. Revised effective ionic-radii and systematic studies of interatomic distances in halides and chalcogenides. Acta Crystallogr. A 32:751–767.

Spandler, C.; Hermann, J.; Arculus, R.; and Mavrogenes, J. 2003. Redistribution of trace elements during prograde metamorphism from lawsonite blueschist to eclogite facies: implications for deep subduction-zone processes. Contrib. Mineral. Petrol. 146:205–222.

Stalder, R.; Foley, S. F.; Brey, G. P.; and Horn, I. 1998. Mineral aqueous fluid partitioning of trace elements at 900–1200°C and 3.0–5.7 GPa: new experimental data for garnet, clinopyroxene, and rutile, and implications for mantle metasomatism. Geochim. Cosmochim. Acta 62:1781–1801.

Sun, S. S., and McDonough, W. F. 1989. Chemical and isotopic systematics of oceanic basalts: implications for mantle composition and processes. *In* Saunders, A. D., and Norry, M. J., eds. Magmatism in the ocean basins. Geol. Soc. Lond. Spec. Publ. 42:313–345.

Sun, W. D. 2003. The subduction factory: a perspective from rhenium and trace element geochemistry of oceanic basalts and eclogites. PhD thesis, Australian National University, Canberra.

Sun, W. D.; Williams, I. S.; and Li, S. G. 2002. Carboniferous and Triassic eclogites in the western Dabie Mountains, east-central China: evidence for protracted convergence of the North and South China Blocks. J. Metamorph. Geol. 20:873–886.

Tiepolo, M.; Vannucci, R.; Oberti, R.; Foley, S.; Bottazzi, P.; and Zanetti, A. 2000. Nb and Ta incorporation and fractionation in titanian pargasite and kaersutite: crystal-chemical constraints and implications for natural systems. Earth Planet. Sci. Lett. 176:185–201.

Tomkins, H. S.; Powell, R.; and Ellis, D. J. 2007. The pressure dependence of the zirconium-in-rutile thermometer. J. Metamorph. Geol. 25:703–713.

Tu, X. L.; Zhang, H.; Deng, W. F.; Ling, M. X.; Liang, H. Y.; Liu, Y.; and Sun, W. D. 2011. Application for RESOlution in-situ laser ablation ICP-MS in trace element analyses. Geochimica 40:83–98.

van der Straaten, F.; Schenk, V.; John, T.; and Gao, J. 2008. Blueschist-facies rehydration of eclogites (Tian Shan,

NW-China): implications for fluid-rock interaction in the subduction channel. Chem. Geol. 255:195–219.

van Westrenen, W.; Blundy, J. D.; and Wood, B. 1999. Crystal-chemical controls on trace element partitioning between garnet and anhydrous silicate melt. Am. Mineral. 84:838–847.

Weyer, S.; Munker, C.; Rehkamper, M.; and Mezger, K. 2002. Determination of ultra-low Nb, Ta, Zr and Hf concentrations and the chondritic Zr/Hf and Nb/Ta ratios by isotope dilution analyses with multiple collector ICP-MS. Chem. Geol. 187:295–313.

Xiao, Y.; Sun, W.; Hoefs, J.; Simon, K.; Zhang, Z.; Li, S.; and Hofmann, A. W. 2006. Making continental crust through slab melting: constraints from niobium-tantalum fractionation in UHP metamorphic rutile. Geochim. Cosmochim. Acta 70:4770–4782.

Xiong, X. L. 2006. Trace element evidence for growth of early continental crust by melting of rutile-bearing hydrous eclogite. Geology 34:945–948.

Xiong, X. L.; Adam, J.; and Green, T. H. 2005. Rutile stability and rutile/melt HFSE partitioning during partial melting of hydrous basalt: implications for TTG genesis. Chem. Geol. 218:339–359.

Xiong, X. L.; Keppler, H.; Audétat, A.; Gudfinnsson, G.; Sun, W. D.; Song, M. S.; Xiao, W. S.; and Li, Y. 2009. Experimental constraints on rutile saturation during partial melting of metabasalt at the amphibolite to eclogite transition, with applications to TTG genesis. Am. Mineral. 94:1175–1186.

Xu, S. K. 2006. Forming and changes of the ore rock in rutile mineral and the relation to the mineralization, Dafushan. Geol. Chem. Miner. 28:73–104.

Xu, S. T.; Su, W.; Liu, Y. C.; Jiang, L. L.; Ji, S. Y.; Okay, A. I.; and Sengör, A. M. C. 1992. Diamond from the Dabie Shan metamorphic rocks and its implication for tectonic setting. Science 256:80–82.

Ye, K.; Cong, B. L.; and Ye, D. I. 2000. The possible subduction of continental material to depths greater than 200 km. Nature 407:734–736.

You, Z. D.; Su, S. G.; Liang, F. H.; and Zhang, Z. M. 2005. The metamorphic evolution of the eclogitic rocks in the main hole of the Chinese Continental Scientific Drilling Project: an elucidation on the uplift processes of the ultrahigh-pressure metamorphic terrane. Acta Petrol. Sin. 21:381–388.

Zack, T., and John, T. 2007. An evaluation of reactive fluid flow and trace element mobility in subducting slabs. Chem. Geol. 239:199–216.

Zack, T.; Kronz, A.; Foley, S. F.; and Rivers, T. 2002. Trace element abundances in rutiles from eclogites and associated garnet mica schists. Chem. Geol. 184:97–122.

Zeng, L. S.; Zhang, Z. M.; Liu, F. L.; and Liang, F. H. 2007. Limited migration and nearly in-situ redistribution of non-conservative elements in retrograde Sulu ultrahigh pressure eclogites. Acta Petrol. Sin. 23:3215–3220.

Zhang, B. R.; Zhang, H. F.; Gao, S.; and Kuang, S. P. 2005*a*. Geochemical architecture of the Dabieshan orogenic belt: ultrahigh-pressure metamorphism and collisional dynamics of the Dabie Mountains. Beijing, Science, p. 118–158.

Zhang, R. Y., and Liou, J. G. 1996. Coesite inclusions in dolomite from eclogite in the southern Dabie Mountains, China: the significance of carbonate minerals in UHPM rocks. Am. Mineral. 81:181–186.

Zhang, R. Y.; Liou, J. G.; and Cong, B. L. 1995. Talc-bearing, magnesite-bearing and Ti-clinohumite-bearing ultrahigh-pressure meta-mafic and ultramafic complex in the Dabie Mountains, China. J. Petrol. 36: 1011–1037.

Zhang, R. Y.; Liou, J. G.; and Ernst, W. G. 2007. Ultrahigh-pressure metamorphic belts in China: major progress in the past several years. Int. Geol. Rev. 49:504–519.

Zhang, Z. M.; Shen, K.; Sun, W. D.; Liu, Y.-S.; Liu, J. G.; Shi, C.; and Wang, J. L. 2008. Fluids in deeply subducted continental crust: petrology, mineral chemistry and fluid inclusion of UHP metamorphic veins from the Sulu orogen, eastern China. Geochim. Cosmochim. Acta 72:3200–3228.

Zhang, Z. M.; Xiao, Y. L.; Liu, F. L.; Liou, J. G.; and Hoefs, J. 2005*b*. Petrogenesis of UHP metamorphic rocks from Qinglongshan, southern Sulu, east-central China. Lithos 81:189–207.

Zhang, Z. M.; Xiao, Y. L.; Shen, K.; and Gao, Y. J. 2005*c*. Garnet growth compositional zonation and metamorphic P-T path of the ultrahigh-pressure eclogites from the Sulu orogenic belt, eastern central China. Acta Petrol. Sin. 21:809–818.

Zhang, Z. M.; You, Z. D.; and Han, Y. J. 1994. High-pressure and very high-pressure metamorphic belt of Tongbai-Dabie area, central China. Earth Sci. J. 19:1–7.

Zhang, Z. M.; Zhang, J. F.; You, Z. D.; and Shen, K. 2005*d*. Ultrahigh-pressure metamorphic P-T-t path of the Sulu orogenic belt, eastern central China. Acta Petrol. Sin. 21:257–270.

Zhao, Z. F.; Zheng, Y. F.; Chen, R. X.; Xia, Q. X.; and Wu, Y. B. 2007. Element mobility in mafic and felsic ultrahigh-pressure metamorphic rocks during continental collision. Geochim. Cosmochim. Acta 71:5244–5266.

Zhong, Z.; Suo, S. T.; and You, Z. D. 1999. Regional-scale extensional tectonic pattern of ultrahigh-P and high-P metamorphic belts from the Dabie massif, China. Int. Geol. Rev. 41:1033–1041.